Packings of 3D stars: stability and structure

Yuchen Zhao, Kevin Liu, Matthew Matthew Zheng, Jonathan Barés, Karola Dierichs, Achim Menges, Robert Behringer

Packings of 3D stars: stability and structure

Yuchen Zhao[1] · **Kevin Liu**[2] · **Matthew Zheng**[3] · **Jonathan Barés**[1] · **Karola Dierichs**[4] · **Achim Menges**[4] · **Robert P. Behringer**[1]

Received: 25 November 2015

Abstract We describe a series of experiments involving the creation of cylindrical packings of star-shaped particles, and an exploration of the stability of these packings. The stars cover a broad range of arm sizes and frictional properties. We carried out three different kinds of experiments, all of which involve columns that are prepared by raining star particles one-by-one into hollow cylinders. As an additional part of the protocol, we sometimes vibrated the column before removing the confining cylinder. We rate stability in terms of r, the ratio of the mass of particles that fall off a pile when it collapsed, to the total particle mass. The first experiment involved the intrinsic stability of the column when the confining cylinder was removed. The second kind of experiment involved adding a uniform load to the top of the column, and then determining the collapse properties. A third experiment involved testing stability to tipping of the piles. We find a stability diagram relating the pile height, h, versus pile diameter, δ, where the stable and unstable regimes are separated by a boundary that is roughly a power-law in h versus δ with an exponent that is less than unity. Increasing vibration and friction, particularly the latter, both tend to stabilize piles, while increasing particle size can destabilize the system under certain conditions.

Keywords Granular · Cylindrical packing · Star-shaped particle · Stability · Friction · Vibration · Aggregate

This article is part of the Topical Collection on Jamming-Based Aleatory Architectures.

✉ Yuchen Zhao
yz172@phy.duke.edu

Jonathan Barés
jb@jonathan-bares.eu

[1] Department of Physics and Center for Nonlinear and Complex Systems, Duke University, Durham, NC, USA

[2] Julia R. Masterman Laboratory and Demonstration School, Philadelphia, PA, USA

[3] North Carolina School of Science and Mathematics, Durham, NC, USA

[4] Institute for Computational Design, University of Stuttgart, Stuttgart, Germany

Published online: 04 April 2016

1 Introduction

Shape is one of the key features of a particle in determining mechanical behavior of an aggregate [1–4]. More particularly, aggregates made from non-convex particles are an emerging area of research that involves tuning material properties to give specific functions to the macroscopic system [5–7]. This is of high interest not only in granular science [4,5] but also for architectural design [8]. Non-convex particle geometries are one main group within the overall area of designed aggregates, in addition to double-non-convex hook-like, convex or even actuated particles [4,9]. These approaches are promising for future lightweight and reversible structural applications. Indeed, such systems can be custom-designed for specific mechanical properties [1,5] and architectural applications. Aggregate systems of particles can also be programmable. The relevance of these synthetic aggregate systems to construction is twofold: on the one hand they can be fully re-configured and re-cycled; on the other hand these structures can be functionally calibrated and graded according to specific mechanical performance criteria.

Two of the most striking characteristics of non-convex designed granulates, in terms of the granular system and possible design applications are their ability to form vertical structures with a 90° angle of repose, and to sustain small

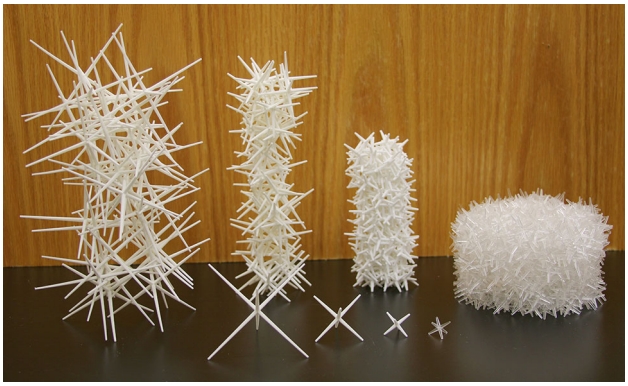

Fig. 1 (color online) Non-convex particles used for experiments. From *left to right* laser sintered white nylon PA2200 particles with size *s* 10, 5 and 2.5 cm and cast acrylic particles of size 2 cm. Each *star* consists of six orthogonal square beams that taper from a thickness of 2 mm at the center of the particle to 1 mm at the tips

tilting or loading perturbations. The aim of this paper is to investigate, in a laboratory setting, how geometry, material, and proportions, as well as preparation and base properties affect the stability of vertical columns. These data serve to inform the production of full-scale architectural construction systems, which integrate mass-production and on-site robotic construction [8].

Aggregate matter made of non-convex particles is also of interest in terms of cohesive strength [4]. This has been investigated in studies of particles that are shaped like staples [4,9,10]. In this paper we investigate the stability of star-shaped particle aggregates. Some research has been done on the packing of such particles [11–13] but little is known about the stability of such aggregates. In the first part, we present our experimental set-ups and the processes used to prepare cylindrical packings. In the second part of this work, results on the intrinsic stability of these aggregates is presented for different particle dimensions and materials, for cylinder aspect ratios, and preparation processes. The effect of vertical loading or tilting is also studied, as well as destabilization due to the inclusion of beads in the packing. Finally these results are discussed in the third part, and rules for a better architectural design are extracted.

2 Experimental set-up

We prepared cylindrical columns in several different ways and subjected them to several different types of perturbations. We used four kinds of stars also called hexapods, that were made from two different types of materials, as shown in Fig. 1. Each star consisted of six orthogonal beams with square cross section, that tapered from a thickness of 2 mm at the center of the particle to 1 mm at the tips. The end-to-end size varied from 2 to 10 cm. They are made of either cast acrylic, which has a friction coefficient 0.4 ± 0.1 or of laser-sintered white nylon PA2200, which has a friction coefficient 1.0 ± 0.3. Since we are here focusing on the issue of pile stability, most experiments were carried out with acrylic particles. Columns made with this type of particle are less stable due to lower friction. Hence, it permits one to observe the limit of stability with relatively small piles. This does not limit the generality of the results since, from a qualitative point of view observations made for low friction particles can be transposed to higher friction ones. In some cases, we also created configurations that were a mixture of stars and beads. The latter were made of acrylic and have a diameter of 9.5 mm and a mass of 0.53 g. We summarize all particle properties in Table 1.

Table 1 Properties of the 3D non-convex particles

Maximum size (cm)	Material	Mass (g)	Friction coefficient
2	Acrylic	0.15	0.4
2.5	Nylon	0.22	1
5	Nylon	0.45	1
10	Nylon	0.84	1

We carried out three kinds of experiments, all of which had the same preparation protocol. The protocol consisted of filling thin-walled tubes with particles by dropping them one-by-one at a steady rate from an overhead hopper that was located 40 cm above a base plate, as shown in Fig. 2a. Each tube was a 30 cm tall PVC pipe whose inner diameter, δ, varied from 2.6 to 20.2 cm. The tubes rested on base plates made of glass for low friction (friction coefficient between glass and acrylic particle is $\sim$0.5) or glass covered with foam for high friction (friction coefficient is higher than the limit of our experimental measurement method, e.g. $\sim$10). During the filling process, the system could be vibrated by an eccentric, driven by a DC motor that was attached to the outside of the tube at a height of $\sim 1.5 \cdot \delta$. We tuned the speed of the motor to create a $\sim$1700 m/s^2 cyclic acceleration of the 16 g eccentric. We measured the height, h, of the pile inside the cylinders by gently dropping a disc of paper on top of the particle packing and measuring the distance between the center of this disc and the base. We removed this disc before the next step.

As shown in Fig. 2b, the tube was then carefully and slowly removed by lifting it vertically. Friction between the particles and the cylinder was low enough not to significantly perturb particles inside the cylinder. This was particularly true for the smaller stars, even when the cylinder diameters were small. For the large, 25mm nylon stars, particles could be dragged by the walls, but this was still a relatively rare occurrence, and columns made of them were highly stable during lifting of the tube.

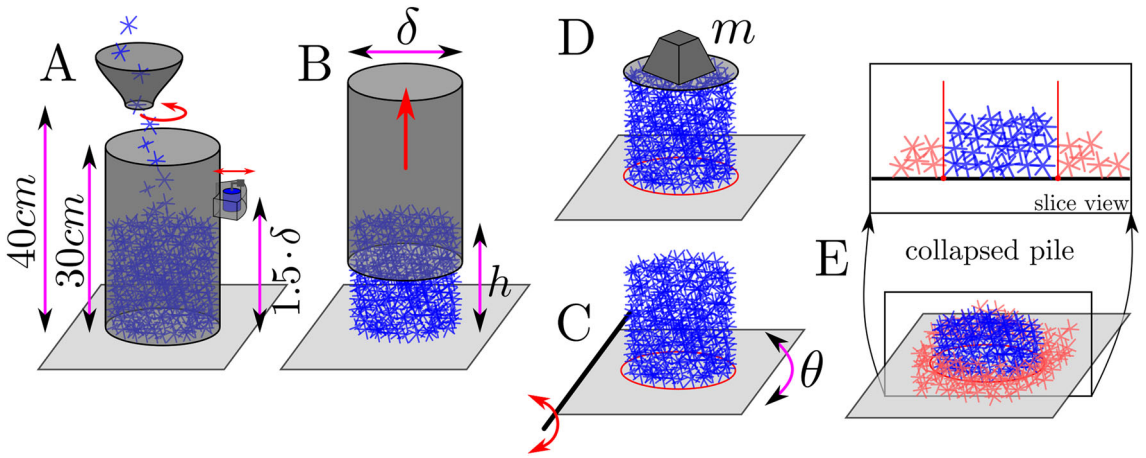

Fig. 2 (color online) **a** Non-convex particles are dropped one-by-one at a Steady rate from an overhead hooper maintained at a constant height in a cylinder of diameter δ and height 30 cm. The system can be vibrated by an eccentric, driven by a DC motor that is attached to the cylinder at a height of $\sim 1.5 \cdot \delta$. **b** Then the pile height, h is measured and the cylinder is carefully and slowly removed by lifting it vertically. **c** If the pile is stable, this stability is tested by tilting the base of an angle θ until the system collapse. **d** The stability is also tested by gradually increasing the mass m of a plate on top of the pile. **e** When the system collapse particles away from the initial cylinder volume (*red* particles) are weighted to quantify the intensity of the collapse. A slice view of the middle of the packing is shown to clarify the geometry. See text for details

In the first kind of experiment, the aim was to study the basic stability of piles. To this end, the tube containing the particles was gently removed. As a quantitative measure of stability, we measured the mass of particles that fell from the column. Figure 2e shows the method we used to quantify the degree of the collapse of a pile: after the cylinder was removed, all particles (red markers in Fig. 2e) lying outside the circle made by the intersection of the cylinder and the base (red circle) were weighed, and their mass was compared to the total mass of the pile (blue and red markers) to compute a collapse ratio:

$$r = \frac{\text{mass of collapsed particles}}{\text{total mass}} \tag{1}$$

When the column was stable, r was close to zero, and when it was unstable, it approached 1. In this paper stability is not considered as a binary situation (either collapsed or not) but more like a progressive variation of the number of 'collapsed' particles. Depending on the use made of the results presented, the reader can choose a threshold value of r to binarise the stability concept. The ratio r is the mass counterpart of the space ratio defined in [14–16] to quantify the intensity of collapse. In our experiments, the particles that fell off did not generally assume a regular shape, hence the need to have a quantitative measure such as r that did not depend on geometry.

In the second kind of experiment, we studied the stability of the piles to tilting. A stable system (meaning no, or very few, particles falling off after the cylinder was removed) was prepared without vibration, on a foam-covered base (high friction). The base was then slowly tilted from horizontal to an angle θ as in Fig. 2c. We found that collapses occurred via small nucleation events, where one or a few particles fell off, which led quickly to a massive collapse that destroyed the main structure of the pile. We measured the angles, θ, for the first nucleation event and the last massive collapse, and computed the collapse ratio, r, for the final event.

A third kind of experiment was carried out to quantify the stability when the piles were loaded vertically. Like the other experiments, we first prepared a stable pile on a glass plate without vibration. We then added a weight to the top (see Fig. 2d) until it collapsed. To do so, we first placed a lightweight rigid disc on top of the pile to distribute the mass. We then placed an empty container on the disc. Finally, we slowly filled the container with water until the pile collapsed. We determined the weight, m, of the filled container plus rigid disc at the time of collapse as a function of the pile height h.

To account for the statistical variability, each set of experiments was repeated at least 10 times to produce an averaged result. All experimental data presented here are mean values, with error bars reflecting the variance over trials. In some cases, these error bars are too small to see. Table 2 summarizes the different experiments.

3 Results

3.1 Intrinsic stability of the pile

In Fig. 3a, we present the evolution of r as a function of h for different cylinder diameters δ. For a given δ, r varies from $r = 0$ (the pile is stable for low height) to $r \simeq 1$ (the pile is fully collapsed) with a reasonably well defined transition between the two behaviors. The relative sharpness of the transition

Table 2 Parameters used for the three kinds of experiment: stability, tilting and loading

$\mathcal{N}$	Test	Stars	Vibration	Basis	δ (cm)	h (cm)	δ/s	h/s
1	Stability	Acrylic 2 cm	No	Glass	4 → 15.4	2.5 → 27.5	2 → 7.7	1.25 → 13.75
2	Stability	Acrylic 2 cm	Yes	Glass	4 → 15.4	2.5 → 27.5	2 → 7.7	1.25 → 13.75
3	Stability	Acrylic 2 cm	No	Foam	7.7 ; 15.4	2.5 → 27.5	3.85 ; 7.7	1.25 → 13.75
4	Stability	Nylon 2.5 cm	No	Glass	4 → 10.1	6 → 30	1.6 → 4.04	2.4 → 12
5	Stability	Nylon 2.5 cm	Yes	Glass	4 → 10.1	6 → 30	1.6 → 4.04	2.4 → 12
6	Stability	Nylon 5 cm	No	Glass	7.7 ; 15.4	7 → 30	1.54 ; 3.08	1.4 → 6
7	Stability	Nylon 10 cm	No	Glass	7.7	12 → 30	0.77	1.2 → 3
8	Stability	Acrylic + beads	No	Glass	13	12.5 ± 3 %	6.5	6.25 ± 3 %
9	Tilting	Acrylic 2 cm	No	Foam	13	8 → 19.5	6.5	4 → 9.75
10	Tilting	Nylon 2.5 cm	No	Foam	15.4	19	6.16	7.6
11	Tilting	Nylon 5 cm	No	Foam	15.4	19	3.08	3.8
12	Tilting	Nylon 10 cm	No	Foam	15.4	19	1.54	1.9
13	Loading	Acrylic 2 cm	No	Glass	13	13.5 → 18.6	6.5	6.75 → 9.3

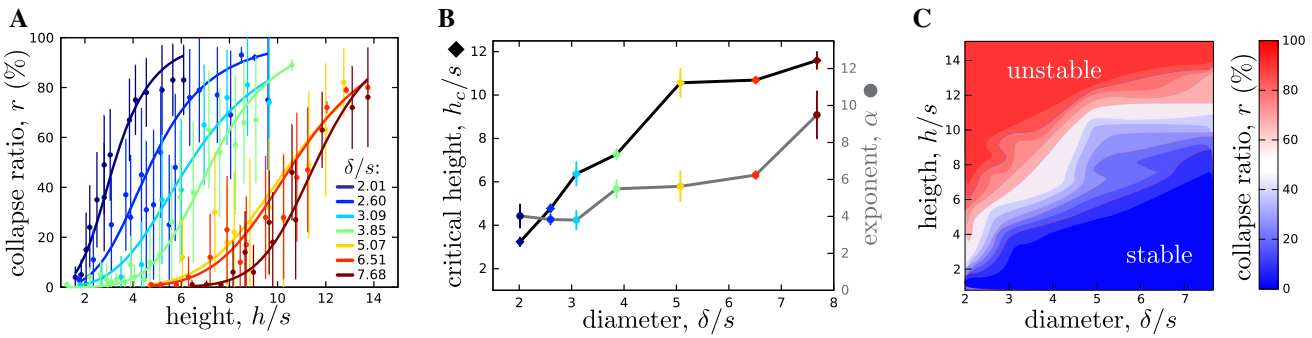

Fig. 3 (color online) Stability of the acrylic particles from experiment $\mathcal{N}1$. **a** ratio r of collapsed particles as a function of the pile height h normalized by the particle size, $s = 2$ cm for different heights of acrylic particle piles and different cylinder sizes δ/s. For each height, the ratio r is averaged over at least 10 realizations and an error-bar is deduced. *Plain curves* are the fit of the data with Eq. 2. **b** Fit parameters h_c (*plain black line*) and α (*grey dashed line*) for different pile diameters δ. **c** Stability phase diagram for acrylic particles. The ratio r of collapsed particles is plotted as a function of the normalized pile height h/s and the normalized pile diameter δ/s. Stable domain is where r is the lowest

means the range of partially stable systems is very narrow: in most cases when a part of the pile begins to collapse, stability is lost for the full structure. In order to characterize this transition and to quantitatively measure the transition height h_c we have fitted the experimental data for $r(h)$ to:

$$r = \frac{1}{\left(\frac{h_c}{h}\right)^{\alpha} + 1}, \tag{2}$$

where h_c is the height for which $r = 1/2$. This expression indicates a critical height, h_c. For large diameters, $r \to 1$ slowly since some particles remain in the original region covered by the uncollapsed pile (red disc in Fig. 2e) after the collapse.

Fitted values of h_c and α for different δ from experiment $\mathcal{N}1$ are presented in Fig. 3b. As suggested qualitatively by Fig. 3a, h_c increases almost linearly with δ and then saturates around a height equivalent to 11 particle lengths (arm-tip-to-arm-tip along an axis). Similarly to what has been done in [17] Fig. 3c shows the extrapolated values of the collapse ratio $r(\delta, h)$ as a function of h, and gives a stability diagram indicating the pile behaviour: stability is greater when δ is large, and an increase does not necessarily significantly improve the stability.

We also consider the effect on stability of the particle geometry, the properties of the base, and the preparation. In Fig. 4, we plot $r(h)$ from experiments $\mathcal{N}1$, 2, 3, 4, 6 and 7 for $\delta = 7.7$ cm and $\delta = 15.4$ cm, for the following configurations:

- 2 cm acrylic particles with the two substrate: slippery glass or rough foam.
- 2 cm acrylic particles on glass with or without vibration.
- slippery 2 cm acrylic particles or rough 2.5 cm nylon particles.
- nylon particles, changing the arm length: 2.5, 5 or 10 cm

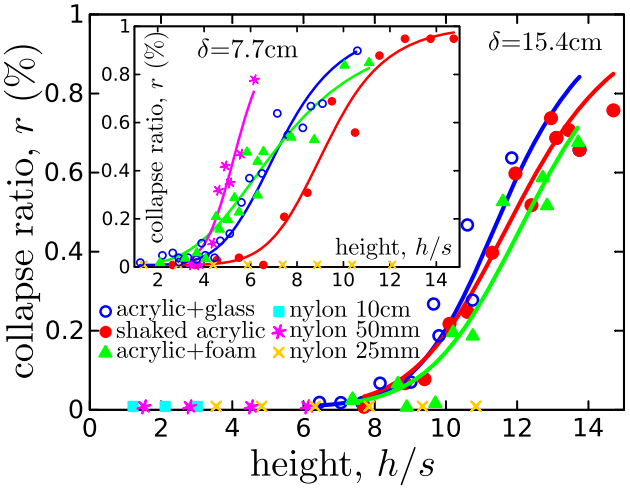

Fig. 4 (color online) Ratio r of collapsed particles as a function of the scaled cylinder height h/s for two different cylinder diameters: $\delta = 7.7$ cm for the inset graph and $\delta = 15.4$ cm for the main panel. In both cases, experiments were made in different situations: (*blue*) acrylic 2 cm particles on a slippery glass base (experiment $\mathcal{N}1$), (*red*) vibrated acrylic particles on glass (experiment $\mathcal{N}2$), (*green*) acrylic particles on a rough foam base (experiment $\mathcal{N}3$), (*cyan/purple/yellow*) nylon 10/5/2.5 cm particles on glass (experiment $\mathcal{N}4$, 6, 7). *Plain curves* were fitted with Eq. 2 and *error-bars* have been removed by sake of clarity

Figure 4 shows that there is only a slight increase of the pile stability when the base is changed from glass with friction coefficient ~0.5 to foam with friction coefficient higher than 10. Hence, the frictional coefficient of the substrate does not influence the pile stability significantly. However, as shown in the inset of Fig. 4, vibrating the system during the preparation measurably increases the stability of the pile by shifting the ratio curve rightward. As shown in the main panel, this effect is weaker for higher pile diameters. This stabilization effect may be due to the fact that in the case of larger δ, more particles are poured, which acts in a similar manner to externally applied vibration.

Figure 4 shows that increasing the friction coefficient between particles (from 0.4 to 1) dramatically increases the value of the critical height h_c. Note that the size difference between acrylic (2 cm) and nylon (2.5 cm) particles is too small to affect stability. Even with the smaller tube ($\delta = 7.7$ cm), we did not observe instability for our tallest piles ($h_c = 30$ cm) for 2.5 cm nylon particles, whereas $h_c \simeq 14$ cm for acrylic particles. We did not observe any stabilisation effect due to the particle size, but the inset of Fig. 4 shows that 5 cm nylon particles are less stable than 2 cm acrylic stars, even if the friction coefficient is larger and the arms longer. This is only observed for $\delta = 7.7$ cm, and is due to the fact that the diameter of the pile is comparable to the particle size. The base of the structure is reduced to too few particles to be stable.

To more accurately analyse the effect of the particle roughness and vibration, Fig. 5c and E show the stability phase diagram for vibrated piles of 2 cm acrylic particles and 2.5 cm nylon particles from experiments $\mathcal{N}2$ and $\mathcal{N}4$ respectively. Fits of Eq. 2 to the data yield $h_c(\delta)$ for these two configurations, as in Fig. 5a.

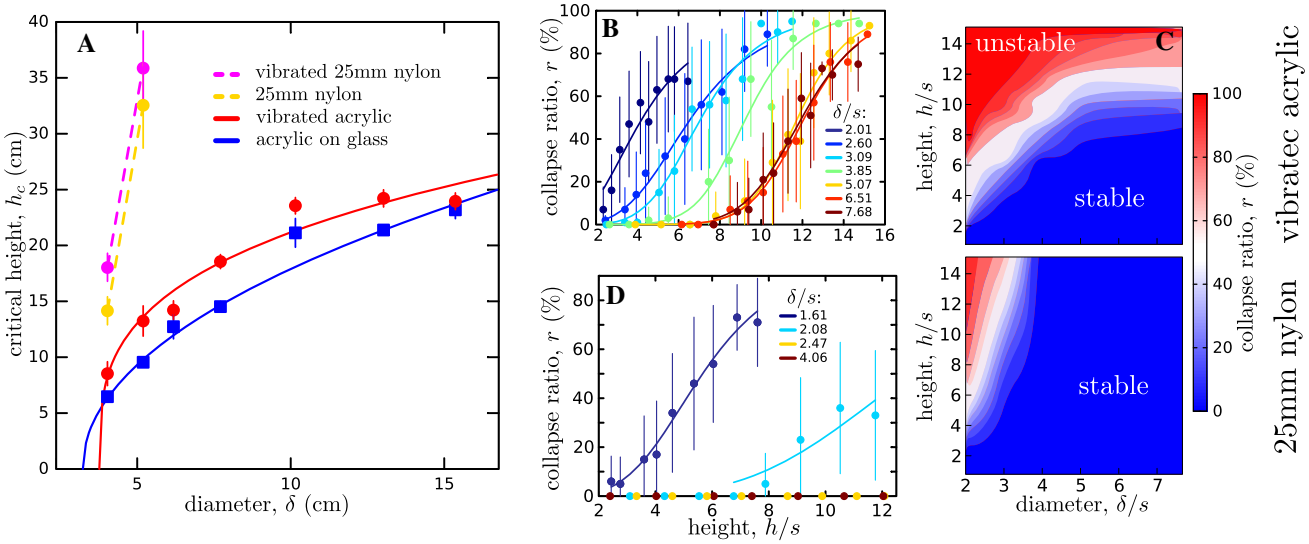

Fig. 5 (color online) Effect of vibration and friction on stability, for experiments $\mathcal{N}1$, 2, 4, 5 **a** Critical stability height hc measured from the fitting of Eq. 2 as a function of the cylinder diameter δ for different packing configurations: vibrated (*red*) and not vibrated (*blue*) 2 cm acrylic particles on glass, vibrated (*pink*) and not vibrated (*yellow*) 2.5 cm Nylon particles on glass. *Plain lines* are *curves* fitted with Eq. 3. **b/d**: ratio r of collapsed particles as a function of the pile height h normalized by the particle size s for different height of vibrated acrylic/2.5 cm nylon particle piles and different cylinder sizes δ/s. Plain curves are the fit of the data with Eq. 2. **c** Stability phase diagram for vibrated acrylic particles. **e** Stability phase diagram for vibrated 2.5 cm nylon particles. The ratio r of collapsed particles is plotted as a function of the normalized pile height h/s and the normalized pile diameter δ/s

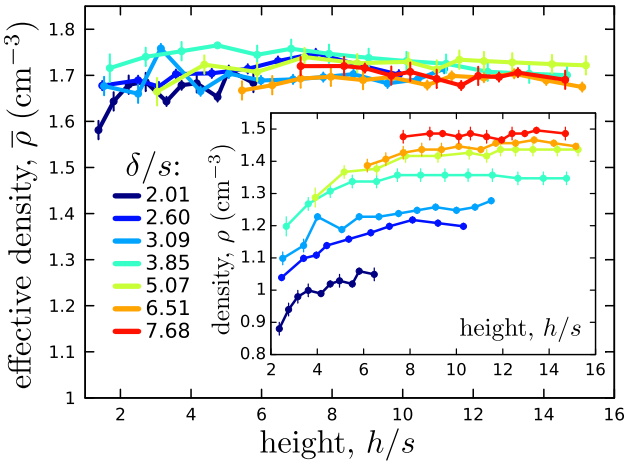

Fig. 6 (color online) *Inset* density ρ of vibrated 2 cm acrylic particle piles (particles per cm^3) as a function of the pile height (h/s) for different pile diameters. *Main panel* effective pile density $\overline{\rho}$ measured correcting the side effects according to Eq. 4 with $\Delta_r = 0.75$. Measurements are from experiment $\mathcal{N}2$

As suggested by Figs. 4 and 5a shows that vibration improves the pile stability, even if the effect is weaker for highly frictional particles and for larger δ. Nevertheless, it appears that the system parameter that has the largest effect on the system stability is the the inter-particle friction coefficient. Indeed, these figures confirm that increasing friction between particles dramatically improves the pile stability, whatever the pile dimensions, and very significantly shifts the $h_c(\delta)$ curve upward. To provide a quantitative analysis, we fitted these curves to:

$$h_c = K(\delta - s_0)^{\beta}, \tag{3}$$

where K quantifies the overall stability of the packing, β quantifies the effect of the pile diameter and s_0, of the same order of magnitude as the particle size s, gives the smallest possible diameter. We note that K is larger for vibrated systems and for rough particles, and that β is smaller for vibrated systems than for non-vibrated ones.

To better understand the higher stability of vibrated systems, we computed the global density, ρ, of the 2 cm acrylic particle piles for the non-vibrated (experiment $\mathcal{N}1$) and vibrated (experiment $\mathcal{N}2$) systems of different diameters and different heights. In the inset of Fig. 6 these data are plotted ($\rho(h, \delta)$) in the case of vibrated piles. The density seems to vary substantially with δ and saturate only for large height. This is due to boundary effects, since the local density is reduced close to the edges of the cylinder. This can easily be corrected in Eq. 4 by removing part of volume near the edges when computing ρ:

$$\overline{\rho} = \frac{n}{\pi(h - \Delta_r)\left(\frac{\delta - \Delta_r}{2}\right)^2} \tag{4}$$

In Eq. 4, Δ_r quantifies how much of the edge volume must be removed. It is comparable to an arm length, and is computed to optimize the collapse of the data in Fig. 6 ($\Delta_r = 0.75$ cm $\sim$ 3/8·particle size). With this correction, we find that the density is effectively constant, with an average value in the non-vibrated case of $\overline{\rho} = 1.6 \pm 0.04$ cm^{-3}, and in the vibrated case of $\overline{\rho} = 1.7 \pm 0.03$ cm^{-3}. Assuming that particle neighbors are located roughly isotropically, this implies that the average interlocking distance between particles changed from to 3.70 mm to 3.57 mm when the packing was vibrated. Hence, a variation of the interlocking distance as small as 0.13 mm can have a very significant impact on the pile stability as emphasized by Fig. 5.

3.2 Destabilization of piles

In order to study other modes of destabilization, we mixed beads among the particles. The total number of particles in the system was kept constant (2300) but the number ratio between 2 cm acrylic particles and 0.95 cm diameter acrylic beads was varied from 0 to $\sim$ 6% in experiment $\mathcal{N}8$. We chose 0.95 cm diameter beads because their radius corresponds to the length of a particle arm. Such a spherical particle can be completely contained in the arms of a star particle, hence weakening the interlocking of the star particles. Also, the bead volume was low enough not to create a strong height variation as we changed the fraction of beads ($h \approx 12.5$ cm). In Fig. 7, we show that the addition of spheres indeed decreases the stability of the pile by linearly increasing the fraction of collapsed particles to beads in the total packing. Similarly, the fraction of collapsed beads also increases linearly with the total fraction of beads. Nevertheless, beads are always destabilizing, since the collapsed bead fraction is always higher than the collapsed star ratio.

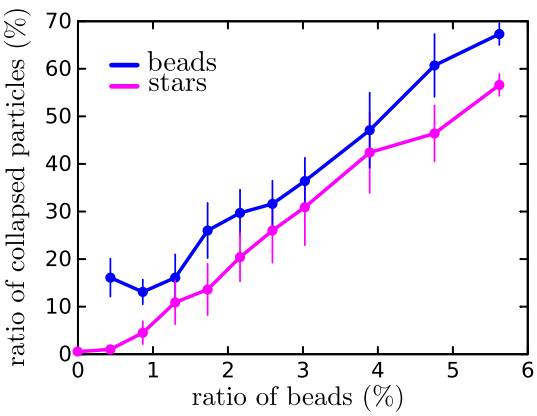

Fig. 7 (color online) Fraction of collapsed beads (0.95 cm diameter acrylic beads) to the total number of beads (*blue*) and ratio of collapsed particles (2 cm acrylic particles) over the total number of particles as a function of the ratio of beads in the 2300 particles packing. Measurements were made from experiment $\mathcal{N}8$

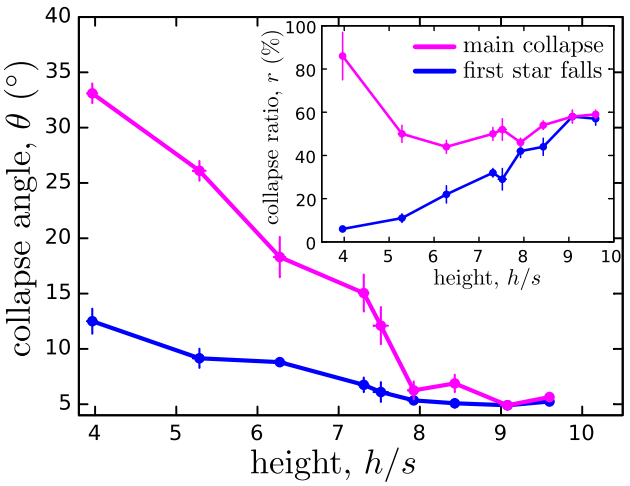

Fig. 8 (color online) Tilt angle θ (see Fig. 2c) for the collapse of the initial particle and for the final collapse as a function of the pile height. *Inset* Collapse ratio r for first and main collapse. Experiments were carried out with 2 cm acrylic particles in a 13 cm diameter cylinder ($\mathcal{N}9$)

Stable systems can also be unbalanced by tilting. Slowly tilting a stable pile of 2 cm acrylic particles induced an initial small collapse of a few particles, corresponding to a small initial rearrangement of the pile. With increasing tilt, this was followed by a series of other small collapses, leading to a final major failure that was system-spanning. The tilting experiment, $\mathcal{N}9$, was carried out with a 13 cm diameter tube on a rough foam substrate for various h. Figure 8 presents the evolution of the initial and final collapse angles, $\theta(h)$ *vs*. h. The initial collapse occurred early in the tilting process and is clearly separated from the last one for low enough h. But, for higher h, the gap between initial and final collapse angles coalesced, and there was only one large collapse. The inset of Fig. 8 shows the ratio of particles lost by the pile after the first and last collapses. As h increased, the angular gap between the two collapses decreased and the ratios of collapsed particles converged, *i.e*. the first and last collapses converge in both angle and intensity. Also, as expected, whether the criterion of stability is the first or last collapse angle, the critical angle rapidly decreased with increasing pile height.

We also carried out tilting experiments with fixed pile sizes ($\delta = 15.4$ cm and $h = 19$ cm) and varying particle sizes. We used nylon particles with arm lengths $s = 2.5$, 5 and 10 cm (experiments $\mathcal{N}10$, 11, 12 respectively). Due to their high friction, nylon particles tended to fall over as a rigid body at the collapse angle, corresponding to an imbalance of the pile center of mass. The final angles of collapse are given in Table 3 which shows that the longer the arms, the less stable the pile. This is due to the fact that the larger the particle, the less contact points there were between the pile and the base and the lower the stability.

Table 3 Angle of collapse for piles with $h = 19$ cm and $\delta = 15.4$ cm and different nylon particle size

Particle size (cm)	Collapse angle (°)
2.5	29.2
5	25.0
10	14.7

Results from experiments $\mathcal{N}10$, 11, 12

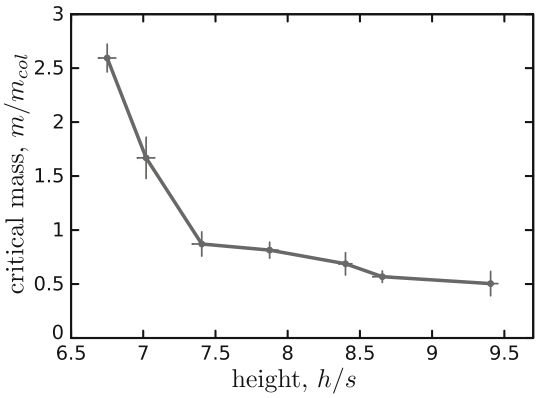

Fig. 9 Maximum mass, m, supported by a stable 13 cm diameter pile before collapsing, as a function of the scaled pile height (h/s). The loading is given as a fraction of the pile mass. Non vibrated 2 cm acrylic particles were used on a glass base (experiment $\mathcal{N}13$)

In the third and last exploration, we prepared piles and then loaded them vertically. Following our previous preparation protocol, we prepared stable piles of 2 cm acrylic particles in a tube of 13 cm diameter, and slowly loaded them vertically. In this case, the collapse happened as a single event at a critical loading mass m. Data for m versus h in Fig. 9 shows that m decreases sharply with h. Also, we note, comparing this graph with data from Fig. 5a, that the mass to make a pile collapse is higher than the mass of additional particles needed to make it collapsed because it is too high. For example, considering the case where $m = m_{col}$ (for $h/h_s \approx 7.4$), if the stabilization process was just a matter of vertical loading, this would mean that h_c should be $h_c/s \approx 15$, whereas Fig. 3 indicates that it is $h_c/s \approx 11$. This implies that a pile does not collapse because it cannot support its own weight, but because of low cohesion of the particles when the pile becomes too high.

4 Discussion and conclusions

We have shown experimentally that star-shaped particles can form stable cylindrical aggregates whose height can be more than three time larger than the base diameter. The stability of these aggregates was tested with and without loading and tilting for particles spaning a broad range of arm sizes and frictional properties. For a given type of star, the column critical height, h_c rapidly increased with the diameter

of the base, δ, when the latter was comparable to the particle size, but plateaued for larger diameters. This means that to increase the height of a cylindrical aggregate one can adjust the base diameter somewhat, but it is more effective to increase the particle size to keep it just smaller than δ. There are other ways to increase the critical height. First, by increasing the friction of the base, the first particle layer is stabilized, which in turn, stabilizes the whole structure. In general, fixing the first layer is a good way to increase the stability of the whole aggregate. Second, by vibrating the system while raining in the particles, the packing fraction increases, and the distance between particles decreases which also enhances stability. This is particularly the case if the system is small, because less shaking energy is required to create rearrangements. Thus, not only is the intrinsic geometry of the system important, but also, the preparation method can improve the aggregate stability. Third, as long as the particle size remains significantly smaller than the pile diameter, using larger particles also increases the stability. But, this effect reverses when the particles become comparable to the cylinder diameter because the effective base of the pile (diameter minus arm length) vanishes. Fourth and finally, the most important parameter for stabilizing a packing, keeping other properties constant (geometry and preparation), is the interparticle friction coefficient. For instance, we found for a given cylinder diameter and particle friction coefficient ~ 1, that a stable aggregate can be more than two times higher than for a friction coefficient of 0.4. Hence, the choice of material or surface properties for the particles for the present experiments is certainly the most important parameter to obtain a tall stable aggregate.

Star-shaped particle aggregates that are stable initially, can sustain destabilization effects, within limits. First, adding a certain fraction of beads with the stars leads to a less stable packing, then when there are no beads. Conversely, it follows that adding non-convex particles to spheres can help stabilize the packing, although we have not investigated the high sphere-fraction limit. Second, stable cylindrical packings collapse via a succession of avalanches when slowly tilted. The collapse angles vary nearly linearly with pile height. This suggests the possibility of creating structures with more complex aggregate geometries, than purely cylindrical and vertical. Third, and finally, a stable packing of star-shaped particles can support up to twice its own weight. However, the ability to support added weight decreases rapidly with pile height.

The data for the acrylic particles constitute a baseline, laboratory-scale exploration, specifically focusing on the issue of pile stability. To create taller, architectural-scale structures, including freestanding walls, arches and domes [8], the same type of star-shaped particles but with higher friction can be used. The results reported in this work represent a step forward in the knowledge of both architectural design and granular science. It gives a better understanding of the self-sustained stability of non-convex 3D particles and their ability to form vertical structures, while it permits a widening of possible design applications. In addition to the scientific aspects, we believe this work constitutes a 'handbook' of mechanical rules to improve the design of aggregated structures by giving methods to make them stronger, more stable and more reliable.

Acknowledgments We thank Dong Wang and Hu Zheng for fruitful discussions and Stephen Teitel and Scott Franklin for a critical review of this manuscript. Y.Z., J.B. and R.P.B. are funded by National Science Foundation (NSF grant DMR-1206351) and W. M. Keck Foundation. K.D. has benefitted from support of ITASCA Educational Partnership Program.

References

1. Miskin, M.Z., Jaeger, H.M.: Evolving design rules for the inverse granular packing problem. Soft Matter **10**(21), 3708–3715 (2014)
2. Athanassiadis, A.G., Miskin, M.Z., Kaplan, P., Rodenberg, N., Lee, S.H., Merritt, J., Brown, E., Amend, J., Lipson, H., Jaeger, H.M.: Particle shape effects on the stress response of granular packings. Soft Matter **10**(1), 48–59 (2014)
3. Smith, K.C., Alam, M., Fisher, T.S.: Athermal jamming of soft frictionless platonic solids. Phys. Rev. E **82**, 051304 (2010)
4. Franklin, S.V.: Extensional rheology of entangled granular materials. Europhys. Lett. **106**(5), 58004 (2014)
5. Miskin, M.Z., Jaeger, H.M.: Adapting granular materials through artificial evolution. Nat. Mater. **12**(4), 326–331 (2013)
6. Saint-Cyr, B., Delenne, J.-Y., Voivret, C., Radjai, F., Sornay, P.: Rheology of granular materials composed of nonconvex particles. Phys. Rev. E **84**, 041302 (2011)
7. Brown, E., Nasto, A., Athanassiadis, A.G., Jaeger, H.M.: Strain stiffening in random packings of entangled granular chains. Phys. Rev. Lett. **108**, 108302 (2012)
8. Dierichs, K., Menges, A.: Granular morphologies: programming material behaviour with designed aggregates. Arch. Des. **85**(5), 86–91 (2015)
9. Gravish, N., Franklin, S.V., Hu, D.L., Goldman, D.I.: Entangled granular media. Phys. Rev. Lett. **108**, 208001 (2012)
10. Franklin, S.V.: Geometric cohesion in granular materials. Phys. Today **65**(9), 70 (2012)
11. Miszta, K., de Graaf, J., Bertoni, G., Dorfs, D., Brescia, R., Marras, S., Ceseracciu, L., Cingolani, R., van Roij, R., Dijkstra, M.: Hierarchical self-assembly of suspended branched colloidal nanocrystals into superlattice structures. Nat. Mater. **10**(11), 872–876 (2011)
12. de Graaf, J., van Roij, R., Dijkstra, M.: Dense regular packings of irregular nonconvex particles. Phys. Rev. Lett. **107**, 155501 (2011)
13. Jiao, Y., Stillinger, F.H., Torquato, S.: Optimal packings of superballs. Phys. Rev. E **79**, 041309 (2009)
14. Lajeunesse, E., Mangeney-Castelnau, A., Vilotte, J.-P.: Spreading of a granular mass on a horizontal plane. Phys. Fluids **16**(7), 2371–2381 (2004)
15. Lube, G., Huppert, H.E., Sparks, R.S.J., Freundt, A.: Collapses of two-dimensional granular columns. Phys. Rev. E **72**, 041301 (2005)
16. Trepanier, M., Franklin, S.V.: Column collapse of granular rods. Phys. Rev. E **82**, 011308 (2010)
17. Desmond, K., Franklin, S.V.: Jamming of three-dimensional prolate granular materials. Phys. Rev. E **73**, 031306 (2006)